Sorbitol is a severity biomarker for PMM2-CDG with therapeutic implications

Journal:	*Annals of Neurology*
Manuscript ID	ANA-21-1042.R2
Wiley - Manuscript type:	Research Article
Date Submitted by the Author:	n/a
Complete List of Authors:	Ligezka, Anna; Mayo Clinic Rochester, Clinical Genomics; Jagiellonian University Medical College, Department of Medical Diagnostics, Faculty of Pharmacy Radenkovic, Silvia; Mayo Clinic Rochester, Clinical Genomics; KUL UZ Gasthuisberg CHROMETA, Department of CHROMETA; KU Leuven Department of Oncology; VIB-KU Leuven Center for Cancer Biology, Metabolomics Expertise Center Saraswat, Mayank; Mayo Clinic Department of Laboratory Medicine and Pathology; Institute of Bioinformatics, International Technology Park Garapati, Kishore; Mayo Clinic Department of Laboratory Medicine and Pathology; Institute of Bioinformatics, International Technology Park, Section of Biochemical Genetics, Division of Human Genetics, Department of Pediatrics Ranatunga, Wasantha; Mayo Clinic Research Rochester, Department of Clinical Genomics Krzysciak, Wirginia; Jagiellonian University Medical College, Department of Medical Diagnostics, Faculty of Pharmacy Yanaihara, Hitoshi; Saitama Medical University, Department of Urology Preston, Graeme; Mayo Clinic Rochester, Department of Clinical Genomics Brucker, William; Rhode Island Hospital, Department of Pediatrics, Human Genetics McGovern, Renee; Mayo Clinic Department of Oncology Reid, Joel; Mayo Clinic College of Medicine and Science, Division of Oncology Research, Department of Oncology Cassiman, David; KU Leuven University Hospitals Leuven, Metabolic Center; KUL UZ Gasthuisberg CHROMETA, Laboratory of Hepatology, Department of CHROMETA Muthusamy, Karthik; Mayo Clinic, Clinical Genomics Johnsen, Christin; Mayo Clinic, Department of Clinical Genomics Mercimek-Andrews, Saadet; University of Alberta Faculty of Medicine & Dentistry, Department of Medical Genetics; The Hospital for Sick Children, Division of Clinical and Metabolic Genetics Larson, Austin; Children's Hospital Colorado, Section of Clinical Genetics and Metabolism, Department of Pediatrics Lam, Christina; Seattle Children's Hospital, Department of Pediatrics, Division of Genetic Medicine; University of Washington School of Medicine, Department of Pediatrics Edmondson, Andrew; CHOP, Section of Biochemical Genetics, Division of Human Genetics, Department of Pediatrics Ghesquiere, Bart; VIB-KU Leuven Center for Cancer Biology, Metabolomics Expertise Center; KU Leuven, Department of Oncology Witters, Peter; KU Leuven University Hospitals Leuven, Metabolic Center; KU Leuven Department of Development and Regeneration, Faculty of Medicine

	Raymond, Kimiyo; Mayo Clinic Department of Laboratory Medicine and Pathology, Biochemical Genetics Laboratory Oglesbee, Devin; Mayo Clinic Department of Laboratory Medicine and Pathology, Biochemical Genetics Laboratory Pandey, Akhilesh; Mayo Clinic Department of Laboratory Medicine and Pathology Perlstein, Ethan; Maggie's Pearl Kozicz, Tamas; Mayo Clinic, Department of Clinical Genomics; Mayo Clinic Department of Laboratory Medicine and Pathology Morava, Eva; Mayo Clinic, Department of Clinical Genomics; Mayo Clinic Department of Laboratory Medicine and Pathology; KU Leuven University Hospitals Leuven, Metabolic Center
Keywords:	PMM2, glycosylation, Epalrestat
Domain:	Translational Medicine

Title: Sorbitol is a severity biomarker for PMM2-CDG with therapeutic implications
Running Head: Sorbitol in PMM2-CDG

Authors: Anna N. Ligezka, MSc[1,2*], Silvia Radenkovic, PhD[1,3,4,5*], Mayank Saraswat, PhD[6,7*], Kishore Garapati, MBBS [6,7,8], Wasantha Ranatunga, PhD[1], Wirginia Krzysciak, PhD[2], Hitoshi Yanaihara, MD, PhD[9], Graeme Preston, PhD[1], William Brucker, MD, PhD[10], Renee M. McGovern, BA[11,] Joel M. Reid, PhD[11], David Cassiman, MD, PhD[12,13], Karthik Muthusamy, MD[1], Christin Johnsen, MD[1], Saadet Mercimek-Andrews, MD, PhD[14,15], Austin Larson, MD[16], Christina Lam, MD[17,18], Andrew C. Edmondson, MD, PhD[19], Bart Ghesquière, PhD[4,5], Peter Witters, MD[12,20], Kimiyo Raymond, MD[6], Devin Oglesbee, MD[6], Akhilesh Pandey, MD, PhD[6], Ethan O. Perlstein, PhD[21], Tamas Kozicz, MD, PhD[1,6], Eva Morava MD, PhD[1,6,12]

[1] Department of Clinical Genomics, Mayo Clinic, Rochester, MN, 55905, USA
[2] Department of Medical Diagnostics, Faculty of Pharmacy, Jagiellonian University Medical College, Medyczna 9, 30-688 Krakow, Poland
[3] Laboratory of Hepatology, Department of CHROMETA, KU Leuven, 3000 Leuven, Belgium
[4] Department of Oncology, KU Leuven, 3000 Leuven, Belgium
[5] Metabolomics Expertise Center, VIB-KU Leuven, 3000 Leuven, Belgium
[6] Department of Laboratory Medicine and Pathology, Mayo Clinic, Rochester, MN USA
[7] Institute of Bioinformatics, International Technology Park, Bangalore 560066, Karnataka, India and Manipal Academy of Higher Education (MAHE), Manipal 576104 Karnataka, India
[8] Center for Molecular Medicine, National Institute of Mental Health and Neurosciences (NIMHANS), Hosur Road, Bangalore 560029, India
[9] Department of Urology, Saitama Medical University, 38, Morohongo, Moroyama-machi, Irumagun, Saitama 350-0495, Japan
[10] Rhode Island Hospital. Department of Pediatrics, Human *Genetics*. Providence, Rhode Island, USA
[11] Division of Oncology Research, Mayo Clinic College of Medicine, Rochester, MN, USA
[12] Department of paediatrics, Metabolic disease center, University Hospitals Leuven, Leuven, Belgium
[13] Laboratory of Hepatology, Department of CHROMETA, KU Leuven, 3000 Leuven, Belgium
[14] Division of Clinical and Metabolic Genetics, The Hospital for Sick Children, Toronto, Ontario, Canada
[15] Department of Medical Genetics, University of Alberta, Stollery Children's Hospital, Alberta Health Services, Edmonton, Alberta, Canada
[16] Section of Clinical Genetics and Metabolism, Department of Pediatrics, University of Colorado School of Medicine, Aurora Colorado
[17] Division of Genetic Medicine, Department of Pediatrics, University of Washington School of Medicine, Seattle, WA, USA
[18] Center for Integrative Brain Research, Seattle Children's Research Institute, Seattle, WA 98101, USA
[19] Section of Biochemical Genetics, Division of Human Genetics, Department of Pediatrics, Children's Hospital of Philadelphia, Philadelphia, PA USA
[20] Department of Development and Regeneration, Faculty of Medicine, KU Leuven, Leuven, Belgium
[21] Maggie's Pearl LLC, 903 Independence Street, Sturgis MI, USA

*** equal authorship contribution**

Corresponding author: Eva Morava, M.D. Ph.D., Department of Clinical Genomics, Mayo Clinic, Rochester, Minnesota, USA, 200 First St SW, Rochester, MN 55905 Morava-Kozicz.Eva@mayo.edu

Text word count: 4500

Title word count: 10

Running head word count: 3

Abstract word count: 250

Introduction word count: 276

Discussion word count: 778

No. of references: 31

No. of tables: 0

No. of figures: 8

No. of color figures: 0 for print

No. of supplementary online tables: 3

Key words: PMM; glycosylation, CDG; sorbitol; therapy

Summary for Social Media If Published

1. *If you and/or a co-author has a Twitter handle that you would like to be tagged, please enter it here. (format: @AUTHORSHANDLE).*
   Ethan Perlstein (@eperlste), Maggie's Pearl LLC (@epalrestat), Eva Morava (@EvaMorava)
2. *What is the current knowledge on the topic? (one to two sentences)*
   Patients with the most common form of congenital disorder of glycosylation (CDG) have a metabolic defect in building sugar chains and placing them on proteins leading to growth delay, balance problems and weakness of the legs called peripheral neuropathy. Epalrestat, a drug used in diabetes showed improvement of the metabolic defect in an animal model of this specific type of CDG, called PMM2-CDG.
3. *What question did this study address? (one to two sentences)*
   We wanted to know whether epalrestat improves the CDG metabolism in patient cells, and whether it is safe and effective in a child with PMM2-CDG who took the drug for a year.
4. *What does this study add to our knowledge? (one to two sentences)*
   We found a metabolite, called sorbitol, which was significantly elevated in severely affected PMM2-CDG patients' urine, especially when they had neuropathic weakness or liver disease. The child with PMM2-CDG on epalrestat treatment showed improvement in balance, growth and in her CDG related metabolic abnormalities during a yearlong treatment.
5. *How might this potentially impact on the practice of neurology? (one to two sentences)*
   PMM2-CDG leads to severe motor disability due to progressive neuropathy and ataxia with no curative treatment options. Epalrestat improves CDG metabolism in patient cells and is a promising drug candidate in Pmm2-CDG patients.

ABSTRACT

Objective: Epalrestat, an aldose reductase inhibitor increases PMM enzyme activity in a PMM2-CDG worm-model. Epalrestat also decreases sorbitol level in diabetic neuropathy. We evaluated the genetic, biochemical and clinical characteristics including the Nijmegen Progression CDG Rating Scale, urine polyol levels and fibroblast glycoproteomics in PMM2-CDG patients.

Methods: We performed PMM enzyme measurements, multiplexed proteomics and glycoproteomics in PMM2-deficient fibroblasts before and after epalrestat treatment. Safety and efficacy of 0.8mg/kg/day oral epalrestat were studied in a child with PMM2-CDG for 12 months.

Results: PMM enzyme activity increased post-epalrestat treatment. Compared to controls, 24% of glycopeptides had reduced abundance in PMM2-deficient fibroblasts, 46% of which improved upon treatment. Total protein N-glycosylation improved upon epalrestat treatment bringing overall glycosylation towards the control fibroblasts' glycosylation profile. Sorbitol levels were increased in the urine of 74% of PMM2-CDG patients and correlated with the presence of peripheral neuropathy, and CDG severity rating scale. In the child with PMM2-CDG on epalrestat treatment, ataxia scores improved together with significant growth improvement. Urinary sorbitol levels nearly normalized in 3 months and blood transferrin glycosylation normalized in 6 months.

Interpretation: Epalrestat improved PMM enzyme activity, N-glycosylation and glycosylation biomarkers in vitro. Leveraging cellular glycoproteome assessment, we provided a systems-level view of treatment efficacy and discovered potential novel biosignatures of therapy response. Epalrestat was well-tolerated and led to significant clinical improvements in the first PMM2-CDG pediatric patient treated with epalrestat. We also propose urinary sorbitol as a novel biomarker for disease severity and treatment response in future clinical trials in PMM2-CDG.

ABBREVIATIONS

ALD	Alcoholic liver disease
ALR2	Aldose reductase
ARI	Aldose reductase inhibitor
AZA	Acetazolamide
CBC	Complete Blood Count
CDG	Congenital disorder(s) of glycosylation
CDG-I	Congenital disorder(s) of glycosylation type I
CNS	Central nervous system
FCDGC	Frontiers in Congenital Disorders of Glycosylation Consortium
ICAM-1	Intercellular Adhesion Molecule 1
ICARS	International cooperative ataxia rating scale
INR	International normalized ratio
IQR	the Interquartile Range
IRB	Institutional Review Boards
LAMP-2	Lysosomal Associated Membrane Protein 2
MPI	Phosphomannose Isomerase
NINDS	Neurological Diseases and Stroke
NPCRS	Nijmegen progression CDG rating scale
PMM	Phosphomannomutase
PMM2	Phosphomannomutase 2
PMM2-CDG	Congenital Disorder of Glycosylation (CDG), Phosphomannomutase Deficiency
RDCRN	Rare Disorders Consortium Disease Network

INTRODUCTION

Congenital disorders of glycosylation (CDG) are a group of inborn error of metabolism affecting the post-translational modifications of proteins and lipids: glycosylation. The most frequent CDG is phosphomannomutase-2 (PMM2)-CDG with an incidence between 1:20 000-1:100 000[1], presenting with developmental delay, ataxia, seizures and hypotonia and frequently with multi-system disease[2]. In most cases, motor disability stems from persistent peripheral neuropathy, combined with muscle weakness and ataxia. Neuropathy progresses already in the first decade of life hindering ambulation[1,3]. There is no curative treatment for PMM2-CDG.

We recently showed that epalrestat increased PMM activity in a worm model of PMM2-CDG[4]. The mechanism of action of epalrestat is not yet understood[4,5]. Epalrestat is a carboxylic acid derivative and a noncompetitive and reversible aldose reductase inhibitor (ARI) used for the treatment of diabetic neuropathy[6,7]. Aldose reductase (ALR2), a key enzyme in the polyol pathway, converts glucose into sorbitol, which is subsequently converted to fructose by sorbitol dehydrogenase (SORD). Aldose reductase plays a crucial role in the development of diabetic peripheral neuropathy[8,9]. Epalrestat is the only commercially available ARI, first approved in Japan in 1992. Long-term treatment with epalrestat demonstrated efficacy in decreasing sorbitol levels in diabetic patients and delayed neuropathy progression without reported complications[10]. A recent study showed that a genetic defect associated with SORD deficiency was associated with elevated sorbitol and hereditary neuropathy[11].

Here, we studied the effect of epalrestat on phosphomannomutase (PMM) enzyme activity in PMM-deficient fibroblasts and leveraged multiplexed glycoproteomics to investigate global cellular N-glycosylation in epalrestat-treated PMM-deficient fibroblasts. Urinary sorbitol excretion was assessed in a cohort of 24 individuals with PMM2-CDG. Finally, we evaluated the safety and efficacy of oral epalrestat therapy in a child with PMM2-CDG.

PATIENTS AND METHODS

1. Prospectively collected clinical and laboratory data in 24 PMM2-CDG patients.

We evaluated the genetic, laboratory, metabolic and clinical data of 24 PMM2-CDG patients (Table S1) enrolled in the Frontier in CDG Consortium (FCDGC) natural history study (*IRB: 19-005187*; https://clinicaltrials.gov/ct2/show/NCT04199000?cond=CDG&draw=2&rank=4).

Disease severity was assessed by Nijmegen Progression CDG Rating Scale (NPCRS), (most severe= 82; Mild (0–14), moderate (15–25) and severe (>26))[12, 13]. P1 was previously reported by Qian et al.[14] and P4 and P5 by Jaeken et al.[15] Patient 1, enrolled in a single IND clinical trial was additionally evaluated by the International cooperative ataxia rating scale (ICARS)[16] (Investigation New Drug Protocol (IND) *PMM2-CDG-001)*. ICARS assesses limb ataxia, dysarthria, posture and gait disturbances, and oculomotor disorders; 0=normal; 100=most severe. We analyzed urinary polyols, including sorbitol and mannitol by gas chromatography/mass spectrometry (GC/MS) in 23 out of 24 PMM2-CDG patients (one patient P6 deceased). We also collected functional *in vitro* data in the fibroblasts of *Patients 1-6, P8, P10, P17, P19, P24* (*IRB: 16-004682*).

2. Effect of epalrestat on PMM enzyme *in vitro*

Patient-derived and control fibroblasts (GM5381, GM5400; GM5757, GM00038, GM8680, GM01863, GM8400 Coriell Institute) were cultured in Minimum Essential Media (MEM; Gibco Carlsbad, CA, USA; 1g/L glucose) supplemented with 10% Fetal Bovine Serum (FBS; Gibco), 10% P/S and maintained in an incubator at 37 °C, 5% CO_2 in the presence and absence of epalrestat for 24 hours[4]. Cells were cultured and harvested by trypsinization with 0.05% Trypsin-EDTA (Gibco). PMM and phosphomannose isomerase (MPI) activity was assayed by spectrophotometric measurements[17]. We evaluated the effect of epalrestat (5 µM, 10 µM or 20 µM) on PMM-deficient fibroblasts of 11 patients (P1-P6, P8, P10, P17, P19, P24) included in the FCDGC natural history study.

3. Effect of epalrestat on glycosylation biomarkers *in vitro*

We used immunoblotting and RT-qPCR to measure ICAM-1 (Intercellular Adhesion Molecule 1), LAMP-2 (Lysosomal Associated Membrane Protein 2) protein and mRNA expression levels, respectively, as cellular markers of N-glycosylation[18,19-21] in 10 PMM-deficient fibroblast lines (P1-P6, P8, P17, P19, P24 (P10 was excluded from this analysis due to inappropriate cell condition)) and controls. Fibroblasts were treated with 10 µM epalrestat (optimal dose based on PMM enzyme activity as described above.

4a. Proteomics and glycoproteomics

Cell were scraped in PBS, pH 7.4 and sonicated with a tip sonicator at 40% amplitude for 3 cycles of 10 seconds each, Equal amount of proteins were digested with trypsin as described previously[22]. The digested peptides were labeled with tandem mass tag (TMT) reagents as per the manufacturer's instructions (ThermoFisher). Labelled samples were pooled into one and either size-exclusion chromatography or basic pH reversed-phase fractionation was performed. An aliquot of dried peptides was resuspended in 100 µL of 0.1% formic acid and injected into Superdex peptide 10/300 column (GE Healthcare). 21 early fractions were collected starting at 10 minutes after injection (total run time of 130 minutes) and analyzed by LC-MS/MS as described previously[22]. Another aliquot of total peptides was cleaned up by C18 TopTips (Glygen) and fractionated by bRPLC on a reversed phase C18 column (4.6 × 100 mm column). 12 fractions were dried and re-suspended in 0.1% formic acid for LC-MS/MS analysis.
A modification of previously published LC-MS/MS parameters[22] were used. Specifically, 21 early fractions from SEC and 12 fractions of bRPLC were analyzed by Orbitrap Exploris480 mass spectrometer (Thermo Fisher Scientific) coupled to an EASY-Spray column (Thermo Fisher Scientific). Every run was 130 minutes with flow rate of 300 nL/min. The gradient used for separation was: equilibration at 3% solvent B from 0 to 4 min, 3% to 10% sol B from 4 to 10 min, 10% to 35% sol B from 10.1 to 125 min, 35% to 80% sol B from 125 to 145 minutes. All experiments were done in DDA mode with top 15 ions isolated at a window of 0.7 m/z and default charge state of +2. Charge states ranging from +2 to +7 were considered for MS/MS events. Stepped collision energy was applied to precursors at normalized collision energies of 15, 25, 40. MS precursor mass range was set to 375 to 2000 m/z and 100 to 2000 for MS/MS. Automatic gain control for MS and MS/MS were 106 and 1 x 105 and injection time to reach AGC were 50 ms and 250 ms respectively. 60 s dynamic exclusion was applied. Data acquisition was performed with option of Lock mass (441.1200025 m/z) for all data.

4b. Database searching and analysis

We used the publicly available software pGlyco Version 2.2.0[23,24]. Glycan database containing 8,092 entries and Uniprot Human Reviewed protein sequences (20,432 entries) were used as proteins sequence fasta file. Cleavage specificity was set to fully tryptic with 2 missed cleavages and precursor and fragment tolerance were set to 5 and 20 ppm. Cysteine carbamidomethylation was set as fixed modification and oxidation of methionine as variable modification. The results

were filtered to retain only entries which had 1% FDR at glycopeptide level. Reporter ion quantification was performed in Proteome Discoverer 2.5 using "reporter ion quantifier" node and Ids were matched with quantitation on a scan-to-scan basis (MS/MS). Proteomics dataset was searched using Sequest in Proteome Discoverer 2.4.

5. Correlation analysis between polyol levels and CDG disease severity, including the presence of neuropathy

We assessed correlation between urine sorbitol and mannitol levels and the severity of NPCRS, patient age, growth, the degree of glycosylation abnormality based on transferrin glycoform analysis, organ-specific scores for liver involvement and severity of the neuropathy according to NPCRS.

6. A Phase I study of epalrestat in a single patient with PMM2-CDG.

Study Design: An open label, single patient (P1) compassionate use study designed to assess the safety and tolerability of oral Epalrestat therapy in a child with PMM2-CDG.

Patient Assessments: Prior to the first dose of epalrestat and at 1, 2, 3, 6, 8, 9, 12 months during treatment, concomitant medications and vital signs were recorded and the patient was evaluated using the NPCRS. In addition, blood was drawn for serum chemistry, hematology, and plasma levels of epalrestat. Urine was collected for polyol measurement at baseline and twice over the course of 12 months of therapy.

Drug administration: Epalrestat was administered orally, 3 times per day (TID) before meals in a divided dose (0.8mg/kg/day; 5 mg TID) of epalrestat (Ono Pharmaceuticals, Osaka, Japan) starting on Day 1 of the Study (*IRB: 19-010017; IND #145262*; Protocol PMM2-CDG-001/A).

Safety and Efficacy: Safety measures included vital signs, change in CBC, liver function (INR, bilirubin, transaminases, and albumin) in blood, change in liver elastography and following the pharmacokinetic profile of epalrestat. The efficacy of epalrestat was studied by clinical follow up (physical exam, NPCRS, ICARS), the standard laboratory tests and transferrin glycoform analysis by mass spectrometry.

Pharmacokinetics: Epalrestat plasma concentrations were measured using an LC-MS/MS assay that was validated according to principles outlined in FDA Guidance Documents. Epalrestat-d5 was utilized as the internal standard. The mass spectrometer was coupled to a Waters Acquity H

class ultra-performance liquid chromatography system (Milford, MA). Data was acquired and analyzed with Waters MassLynx v4.1 software. The chromatographic separation of epalrestat and internal standard was accomplished using an Agilent Infinity Lab Poroshell 120 EC-C18 column, 2.1 x 100 mm, 2.7 µm (ChromTech, Apple Valley, MN) with an Agilent Poroshell 120 EC-C18 precolumn, 2.1 x 5 mm, 2.7 µm (ChromTech, Apple Valley, MN). Plasma samples were analyzed after protein precipitation with methanol, concentration to dryness under nitrogen and reconstitution in methanol:water (1:1 v/v). Pharmacokinetics were estimated by non-linear least squares regression using the program Pheonix Winnonlin.

Urine sample collection: Urine was collected for polyol measurement at baseline and twice over the course of 12 months of therapy (*IRB: 16-004682*).

7. Statistical analyses

All data are expressed as mean±SD. All statistical analyses were performed using either GraphPad Prism 8.3 or JAMOVI v.1.6.9 (https://www.jamovi.org). Two sample t tests were used to compare two groups, while one-way ANOVA was used to compare groups of three or more. Shapiro Wilk test was used for normality. Non-parametric tests (Mann Whitney test for comparing two groups and Kruskal-Wallis Test for three or more groups) were used if dependent variable were not normally distributed. p-value <0.05 was considered significant. Bonferroni p-value correction was applied for multiple comparisons. $p<0.05$(*), $p<0.01$(**), $p<0.001$(***), $p<0.0001$(****). NPCRS scores were collapsed into three categories of mild, moderate, and severe, and correlation coefficients with mannitol and sorbitol measurements were calculated using Pearson's r ($p<0.05$). Liver involvement, already in the form of binary values was correlated with the same approach ($p<0.05$).

RESULTS

1. Prospectively collected clinical data

In the cohort of 16 males and 8 females, mean age was 13 years, (range 1 to 70 years, one male patient (P6) deceased at the age of 7). Nineteen patients were younger than 16 years old and four were adults. Transferrin glycoform ratios were available for 23 patients. The total median NPCRS score of all patients was 23 (moderate phenotype), ranging from 8 to 35: 2 mild, 11

moderate, and 11 severe phenotypes. The most common genotypes were c.422G>A/c.357C>A in three patients, c.422G>A/c.338C>T in three patients and c.422 G>A/c.385G>A in two patients. Overall, the most common pathogenic variant was, as expected, c.422G>A (15/24), followed by c.338C>T (4/24) and c.357C>A (3/24)

Neurological symptoms were the most frequent findings; almost all patients presented with severe developmental disability and cerebellar ataxia (23/24). Most suffered from hypotonia (19/24), neuropathy (14/24) or a movement disorder (8/24), leading to impaired mobility (23/24) and communication skills (22/24). Almost half of the patients (10/24) suffered from seizures and (mostly mild) visual impairment (10/24). 18/24 patients had strabismus. Hearing loss (5/24), spasticity (5/24) and encephalopathy (3/24) were relatively rare. About half of the patients had either coagulation abnormalities (15/24), gastrointestinal symptoms (14/24), endocrine disturbances (10/24) or liver involvement (10/24) (Table S1).

2. Epalrestat increases PMM enzyme activity *in vitro*

Nine out of ten patients showed at least 10% increase of PMM enzyme activity upon either 5 μM, 10 μM, or 20 μM epalrestat treatment. Patients showed up to 50% increase in PMM activity with at least one of three concentrations. Three patients showed the highest PMM enzyme activity when treated with 5 μM epalrestat (43% in P1, 35% in P5, 22% in P10); four exhibited the highest PMM enzyme activity with 10 μM epalrestat (33% in P2, 35% in P3, 16% in P8 and 36% in P24); and three patients showed improved PMM enzyme activity at 20 μM epalrestat (50% in P4, 10% in P17, 20% in P19). Altogether, 80% (8/10) of patient fibroblasts responded to 10 μM epalrestat with 10 to 36% increase in PMM enzyme activity (**Fig 1A,** Table S2). (10 μM epalrestat concentration is comparable to the concentration measured in human blood upon epalrestat treatment).

3. Effect of epalrestat on classical glycosylation biomarkers

ICAM-1 and *LAMP-2* mRNA expression of PMM2-deficient and control fibroblasts were similar (data not shown). Treatment with 10 μM epalrestat had no effect on either *ICAM-1* or *LAMP-2* mRNA expression.

Western blot analysis of PMM-deficient fibroblasts (n=10; P1-P6, P8, P17, P19, P24) revealed that although ICAM-1 was decreased in some individuals, we did not find significant

difference in the abundance of ICAM-1 compared to controls (data not shown). Treatment with 10 μM epalrestat resulted in an increase in ICAM-1 protein expression (p=0.02; **Fig 1B**, **D**). LAMP-2 protein abundance was comparable between PMM-deficient and control fibroblasts before treatment, but all patient fibroblasts showed a "smear pattern" (result of differences in LAMP2 mass due to decreased glycosylation), compared to a single LAMP-2 band in controls (**Fig 1E**). LAMP-2 protein abundance showed a marginal but not significant increase after treatment (**Fig 1C**) and no change in the "smear pattern" (**Fig 1E**).

4a. PMM-deficient fibroblasts exhibit moderate reduction of selected proteins but global reduction in N-glycosylation

Six patient-derived fibroblasts (P1-P6) were treated with epalrestat and paired samples as well as four untreated control fibroblasts were analyzed by deep multiplexed proteomics and glycoproteomics. 6,636 proteins with 61,124 peptides were identified and quantified. We also established the abundances of 6,061 individual intact glycopeptides with 249 unique glycan compositions (554 glycan structures) on 926 glycosylation sites of 494 glycoproteins.

In untreated PMM-deficient fibroblasts, 563 proteins were significantly different from controls. As expected, PMM2 protein levels were reduced 1.6-fold in PMM-deficient fibroblasts compared to controls, while mannose-6-phosphate isomerase was not different. Globally, after imposing the 30% change cutoff (fold change 1.3) as a filter, 147 proteins remained different, of which 102 were reduced in abundance (**Fig 2A, B**). Of note, only 15 proteins had two-fold or more reduced abundance and 3 proteins were increased twofold. Among the notable reduced proteins, prolyl hydroxylase EGLN3, vascular endothelial growth factor receptor 3, fibrinogen beta and gamma chains and tissue factor were identified. The glycoproteome had widespread alterations in PMM-deficient fibroblasts (**Fig 3A, B**), and differential abundance of 1,497 glycopeptides was found, of which 1,448 were reduced compared to controls ($p<0.05$). The global reduction in N-glycosylation is visible in **Fig 3**, in which the volcano plot (**Fig 3B**) is skewed to the left. Out of 1,448 reduced glycopeptides a 30% change cutoff qualified 1,289 glycopeptides to be significantly reduced. The top reduced glycopeptide belonged to aspartyl/asparaginyl beta-hydroxylase (N12, Hex10HexNAc2), which is a calcium sensor in endoplasmic reticulum-plasma membrane junction. The most affected glycoproteins with global reduction in glycosylation were fibronectin (FN, 78 glycopeptides from 5 glycosylation sites),

basement membrane-specific heparan sulfate proteoglycan core protein (HSPG2, 17 glycopeptides from 3 sites), protein-lysine 6-oxidase (LYOX1, 17 glycopeptides from one site, N81), Prolow-density lipoprotein receptor-related protein 1 (LRP1, 14 glycopeptides from 5 sites), CD63 (13 glycopeptides from 1 site, N130) and CD166 (13 glycopeptides from 3 sites). Notably, 36 glycopeptides of LAMP-1 and 16 glycopeptides of LAMP-2 were also markedly reduced. ICAM-1 protein levels were not significantly different between PMM-deficient fibroblasts and controls by proteomics measurements. Additionally, we detected seven complex type glycans at Asn267 of ICAM-1 protein, which followed the same trend of not being significant between the PMM-deficient fibroblasts and controls.

4b. Epalrestat treatment improves global glycosylation profile of PMM-deficient fibroblasts

In paired sample analysis before and after epalrestat treatment of PMM2-CDG patient fibroblasts, proteomic measurements revealed 628 proteins to be different post-treatment which was reduced to only 13 proteins with 30% or bigger change cutoff (**Fig 2C, D**), 12 of which were increased post treatment. Untreated and treated fibroblasts did not show marked changes in protein levels (**Fig 4A, B**). Sorbitol dehydrogenase (SORD) showed a modest 11% increase in abundance, but the reduced PMM2 protein levels did not improve upon epalrestat treatment in any comparison (**Fig 2C**). Looking at the glycoproteome, 412 glycopeptides had differential abundance, with none of them reduced in epalrestat-treated fibroblasts (**Fig 3C, D**). These 412 glycopeptides, which significantly improved in their abundance upon epalrestat treatment (**Fig 3D**), also included 97 glycopeptides which had reduced glycosylation in PMM-deficient fibroblasts compared to controls. Twenty four of these 97 glycopeptides contained high-mannose glycans (Man4-Man9). When treated fibroblasts were compared to untreated controls, 665 of 1,448 glycopeptides (46%), that had reduced abundance in untreated PMM-deficient fibroblasts (PMM2 vs. controls), improved post-treatment, becoming similar to controls. 217 of these glycopeptides contained Man4-Man9 glycans and others had complex/hybrid type glycan structures. One of the complex-type glycans at Asn267 of ICAM-1 protein, which was highly fucosylated at branch in addition to being core-fucosylated (Hex7HexNAc6NeuAc2Fuc5 at Asn267), modestly increased (10%) in abundance in paired epalrestat vs. vehicle analysis. Among the glycoproteins which became similar to controls in glycopeptide abundance upon

treatment, CD63, CD166, LRP1, LAMP-1, LAMP-2, LYOX1, FN, alpha- and beta-integrins, collagen family members, and CD44 were notable. The glycopeptides which showed the greatest improvements are marked in **Fig 5.**

5. Elevated urine sorbitol and mannitol in PMM2-CDG patients with peripheral neuropathy and liver pathology

Urine polyol levels were normal (erythritol, arabinitol, ribitol, galactitol) except for sorbitol and mannitol in most PMM2-CDG patients. Urine sorbitol levels ranged from 2.24 to 41 mmol/mol creatinine (controls; <5 mmol/mol creatinine) and 74% of the PMM2-CDG patients presented with an increased urine sorbitol level (17/23) (Table S1). Urine mannitol levels ranged from 3.64 to 648.6 mmol/mol/creatinine (controls; <20 mmol/mol creatinine), with 61% of the PMM2-CDG patients presenting with increased urine mannitol level (14/23) (Table S1).

Urine concentrations of sorbitol ($p=0.015$) and mannitol ($p=0.001$) were higher in patients with moderate peripheral neuropathy, compared to no neuropathy (**Fig 6A, C**). Urine sorbitol ($p=0.004$) and mannitol ($p=0.02$) was increased in patients with mild liver pathology (elevated transaminases; **Fig 6B, D**). Urine sorbitol levels positively correlated ($r=0.5$) with "severe" ($p<0.02$), but not with mild or moderate category (patient category based on NPCRS severity scores; **Fig 6E**). Mannitol measurements did not correlate with either categories (**Fig 6F**). We found no significant correlation between urine sorbitol or mannitol levels, and age, growth or mono/di-oligo and a-oligo/di-oligo transferrin levels.

6a. Evaluation of the safety and efficacy of epalrestat in a single PMM2-CDG patient

P1 single-dose PK data on 0.27 mg/kg epalrestat three times a day (0.8mg/kg/day) were comparable to doses successfully used in the culture media of patient fibroblasts (this dose is 1/3 of the epalrestat dose used in diabetic adults). No adverse events were reported. All vital signs remained normal throughout the duration of the study. Standard Laboratory Screening was performed; values for CBC with differential (a full blood count), transaminases, bilirubin, and albumin remained normal throughout the study. In addition, antithrombin III levels and International normalized ratio (INR) remained at normal levels throughout the study (data not shown). Liver elastography remained normal. The Interquartile Range to Median ratio prior to

therapy was 14%, after 1 month of therapy was 12%; at 6 months: 20% and at 12 months was at 8% (normal below 25%).

6b. Study measurements showed efficacy across multiple outcome measures:

ICARS; The epalrestat-treated patient's ICARS score improved from a score of 56 to a score of 42 within 12 months. Prior to enrollment, the patient was under treatment for five months with acetazolamide (AZA;[13]), which produced an improvement from ICARS score 66 to score 56 before the start of epalrestat treatment. AZA was discontinued for one month prior to the start of epalrestat dosing. After withdrawal of AZA, patients typically regress to pre-intervention scores within 5-8 weeks [13]. However, treatment with epalrestat not only prevented the expected reversal, but it showed further improvement to an ICARS score of 42.

Growth. The body mass index (BMI) showed a notable improvement without any diet modifications to 18.5 (95th percentile) from its previous trough at 14.8 (30th percentile), mirroring the improved appetite, and potentially improved absorption in a 12-month-follow-up period (**Fig 7A**).

NPCRS. The Rating Scale indicated a minimal improvement from a baseline between 21-24 in the six months period before the trial to a score of 20-21 between Month 6, 9 and 12.

Blood transferrin glycoform analysis. The level of transferrin glycosylation (Mono-oligo:Di-oligo ratio) showed a significant improvement. Before treatment the level was abnormal and ranged from 0.09 to 0.14 (normal < or =0.06). After 6 months of therapy the level of transferrin normalized (0.06 at 6 months; normal < or = 0.06); at the 9th month visit transferrin glycosylation became marginally abnormal (0.09 at 9 months; normal < or = 0.06) while the patient was on suboptimal epalrestat dose due to weight gain and normalized with dose correction (0.06 at 12 months) (**Fig 7E,** Table S3).

Pharmacokinetic profile of epalrestat. A graph of the plasma concentration versus time following an oral dose of epalrestat shows rapid absorption and elimination, mirroring the rapid elimination observed in adults (**Fig 7B**). A peak concentration of 1125ng/ml (3.5 μM) epalrestat in plasma occurred one hour after the epalrestat administration. The trough level as the lowest concentration reached by epalrestat before the next dose was 23.4 ng/ml (0.1 μM) after eight hours. Epalrestat was eliminated with a t½ of ~1.04 hours. The systemic exposure (AUC) and oral clearance after a 5 mg dose of epalrestat were 2792 hr*ng/mL and 1.8 L/hr, respectively.

Urine sorbitol and mannitol on epalrestat therapy; Urine sorbitol and mannitol levels were significantly elevated before therapy in a single patient with PMM2-CDG compared to controls. (**Fig 7C**, **D).** Epalrestat treatment nearly normalized urine sorbitol and mannitol levels compared to controls (**Fig 7C, D**). Improvement in urine sorbitol levels were observed in parallel with biochemical and clinical improvements (**Fig 7E**). Other polyols (erythritol, arabitol, ribitol, galactitol) were normal.

DISCUSSION

Based on animal model data, we hypothesized that epalrestat could be a promising candidate for drug repurposing for PMM2-CDG[6]. First, we evaluated the *in vitro* effects of different concentrations of epalrestat on PMM enzyme activity and the global proteomic and glycosylation profile in PMM-deficient and control fibroblasts. We found that 10μM epalrestat was able to increase PMM enzyme activity and showed an improved global glycosylation profile *in vitro*. As there is no clear correlation between the variants in the *PMM2* gene and differences in dose response, there could be other (genetic) factors affecting the patients' response to epalrestat treatment.

We also assessed two classical glycosylation biomarkers, ICAM-1 and LAMP-2 protein abundance and mRNA expression. ICAM-1 and LAMP-2 gene expressions did not differ between PMM-deficient and control fibroblasts. The magnitude of decreased ICAM-1 protein abundance varied between individuals, but it was not significantly different between PMM-deficient and control fibroblasts (nor was LAMP-2 protein expression). Proteomic measurements confirmed this finding. This was an unexpected finding, as ICAM-1 is a frequently used biomarker in CDG[19,25].

Interestingly, glycoproteomics showed that 16 glycopeptides of LAMP-2 had more than 30% reduction in abundance (PMM2/Controls, fold change<0.76) and a hybrid glycan contained at N356 had 80% reduction (Hex5HexNAc3NeuAc1Fuc1 at N356). Twelve out of these 16 glycopeptides fully recovered post epalrestat treatment (treated PMM-deficient fibroblasts compared to untreated controls $p<0.05$). ICAM-1 protein glycosylation was also modestly increased in abundance upon epalrestat treatment. This suggests that mass spectrometry based site-specific glycosylation analysis is a much more sensitive method in diagnostics as well as monitoring therapy response. Although not all the patients showed a significant increase in

PMM activity *in vitro*, glycoproteomics did show an improvement in glycosylation, suggesting that epalrestat could be beneficial even for patients who only show a minimal therapeutic increase in PMM activity.

The beneficial effects of epalrestat on glycosylation were further supported by a clinical and glycosylation improvement in a single PMM2-CDG patient during a 12-month oral epalrestat treatment. This finding suggests that epalrestat can improve patient glycosylation at achievable plasma concentrations with three times daily dosing. We should note that even in epalrestat "non-responding" patients epalrestat treatment could be considered and might be beneficial with respect to targeting polyol metabolism and decreasing elevated polyol levels.

In line with this observation, 412 glycopeptides increased in abundance *in vitro* upon epalrestat treatment and none decreased. 97 glycopeptides that had reduced abundance compared to controls, improved upon epalrestat treatment (treated vs, untreated). Two glycoproteins alone accounted for 21 of these glycopeptides, Thy1 membrane glycoprotein (CD90) and neuroplastin, both of which are highly glycosylated proteins. While CD90 expression is more restricted to brain and skin, neuroplastin is expressed in several tissues throughout the body. Dysregulation of highly glycosylated proteins has been documented in CDG type I (SRD5A3-CDG)[26] and hypoglycosylation of unidentified proteins in several cell/tissue types is a potential causative factor of clinical presentation of CDG. Modern glycoproteomic techniques such as presented here can fill this gap in understanding of these disorders and provide avenues for potential biomarkers.

Further, we hypothesized the possibility of altered polyol metabolism in PMM2-CDG, and hence the beneficial effects of epalrestat treatment to decrease urine polyol levels. Epalrestat has been used as a therapeutic agent to decrease elevated sorbitol levels in diabetes related neuropathy[27,28]. The ability of epalrestat to safely improve symptoms of neuropathy alone by reducing oxidative stress, increasing glutathione levels, and reducing intracellular sorbitol makes it a desirable medication for patients with chronically elevated sorbitol levels[10,29-31]. Though PMM2-CDG patients do not present with hyperglycemia, a diverted flux towards sugar alcohol (polyol accumulation) production due to a block in the pathway seems likely (**Fig 8**). We therefore evaluated urine polyols, specifically sorbitol and mannitol, in 23 patients. While most metabolites of the trans-aldolase pathway and galactitol were normal in all individuals with PMM2-CDG, sorbitol and mannitol levels were elevated in a majority (74%) of the patients.

Additionally, the urine sorbitol and mannitol levels in a single patient enrolled in the epalrestat study, were significantly elevated at the beginning of the trial and nearly normalized after 3 months of treatment correlating with clinical improvement.

We then evaluated the clinical significance of elevated sorbitol in PMM2-CDG. Given that SORD (sorbitol dehydrogenase) deficiency has been linked to hereditary neuropathy[11] our findings suggest that the increased sorbitol and mannitol levels could be one of the underlying causes of neuropathy in PMM2-CDG. Interestingly, SORD levels modestly increased in PMM-deficient fibroblasts upon epalrestat treatment as revealed by paired samples' analysis. This observation is crucial, as it implicates urine polyol screening should be a part of routine clinical workup for PMM2-CDG and could be an important predictor of disease severity and treatment response in individuals with PMM2-CDG.

CONCLUSION

We propose sorbitol as a novel potential biomarker that could be used as a surrogate endpoint in future clinical trials in individuals with PMM2-CDG. Global glycoproteomic characterization of samples of individuals with PMM2-CDG is an emerging paradigm capable of enhancing our understanding of PMM2-CDG and provide quantitative, clinical-labs-based biomarkers for assessing therapy response. The improvement of PMM enzyme activity, and global glycosylation suggest epalrestat is a rational treatment target for PMM2-CDG and should be tested in a larger clinical trial.

ACKNOWLEDGMENTS

We sincerely thank the patient and her family (Maggie's PMM2-CDG Cure, LLC), as well as Perlara PBC for collaborating on the initial drug repurposing screens and preclinical validation of epalrestat.

This work was funded by the grant titled Frontiers in Congenital Disorders of Glycosylation (1U54NS115198-01) from the National Institute of Neurological Diseases and Stroke (NINDS) and the National Center for Advancing Translational Sciences (NCATS), and the Rare Disorders Clinical Research Network (RDCRN), at the National Institute of Health.

PW was funded by the Fonds Wetenschappelijk Onderzoek - Vlaanderen (Fundamenteel

Klinisch Mandaat 18B4322N)

AUTHORSHIP CONTRIBUTION

SR, MS, HY, EOP, BG, KR, AP, TK: contributed to the study concept and design

KG, WR, GP, JR, DC, KM, SA, ACE, PW, KR, DO: participated in the data acquisition and analysis

ANL, WK, WB, CHJ, AL, CHL, AP, EM: contributed to the drafting of the manuscript

POTENTIAL CONFLICTS OF INTEREST

Mayo Clinic and Eva Morava have a financial interest related to this research. This research has been reviewed by the Mayo Clinic Conflict of Interest Review Board and is being conducted in compliance with Mayo Clinic Conflict of Interest policies. Maggie's Pearl LLC and Ethan Perlstein have a financial interest related to this research. Eva Morava and Mayo Clinic has a "Know How" on Epalrestat treatment development for future clinical trials entitled *Clinical investigations on the safety and efficacy of using oral Epalrestat in Phosphomannomutase 2-congenital disorders of glycosylation*. Ethan Perlstein is the CEO of Maggie's Pearl LLC, which is developing epalrestat for future clinical trials. Maggie's Pearl LLC holds an Orphan Drug Designation for epalrestat, which is in development for the treatment of PMM2-CDG. Ethan Perlstein is also CEO of Perlara PBC.

REFERENCES

1. Altassan, R. *et al.* International clinical guidelines for the management of phosphomannomutase 2-congenital disorders of glycosylation: Diagnosis, treatment and follow up. *J Inherit Metab Dis* **42**, 5-28 (2019).
2. Ferreira, C.R. *et al.* Recognizable phenotypes in CDG. *J Inherit Metab Dis* **41**, 541-553 (2018).
3. Witters, P. *et al.* Long-term follow-up in PMM2-CDG: are we ready to start treatment trials? *Genetics in Medicine* **21**, 1181-1188 (2019).
4. Iyer, S. *et al.* Repurposing the aldose reductase inhibitor and diabetic neuropathy drug epalrestat for the congenital disorder of glycosylation PMM2-CDG. *Disease Models & Mechanisms* **12**, 11 (2019).
5. Monticelli, M., Liguori, L., Allocca, M., Andreotti, G. & Cubellis, M.V. β-Glucose-1,6-Bisphosphate Stabilizes Pathological Phophomannomutase2 Mutants In Vitro and Represents a Lead Compound to Develop Pharmacological Chaperones for the Most Common Disorder of Glycosylation, PMM2-CDG. *International Journal of Molecular Sciences* **20**, 4164 (2019).
6. Sharma, S. & Sharma, N. Epalrestat, an aldose reductase inhibitor, in diabetic neuropathy: An Indian perspective. *Annals of Indian Academy of Neurology* **11**, 231-235 (2008).
7. Haneda, M. *et al.* Japanese Clinical Practice Guideline for Diabetes 2016. *Journal of diabetes investigation* **9**, 657-697 (2018).
8. Pal, P.B., Sonowal, H., Shukla, K., Srivastava, S.K. & Ramana, K.V. Aldose reductase regulates hyperglycemia-induced huvec death via SIRT1/AMPK-alpha1/mTOR pathway. *Journal of Molecular Endocrinology* **63**, 11-25 (2019).
9. Qiu, L., Guo, C. & Hua, B. Aldose Reductase Inhibitors of Plant Origin in the Prevention and Treatment of Alcoholic Liver Disease: A Minireview. *BioMed Research International* **2019**, 3808594 (2019).
10. Hotta, N. *et al.* Long-term clinical effects of epalrestat, an aldose reductase inhibitor, on diabetic peripheral neuropathy: the 3-year, multicenter, comparative Aldose Reductase Inhibitor-Diabetes Complications Trial. *Diabetes Care* **29**, 1538-44 (2006).
11. Cortese, A. *et al.* Biallelic mutations in SORD cause a common and potentially treatable hereditary neuropathy with implications for diabetes. *Nature Genetics* **52**, 473-481 (2020).
12. Achouitar, S. *et al.* Nijmegen paediatric CDG rating scale: a novel tool to assess disease progression. *J Inherit Metab Dis* **34**, 923-7 (2011).
13. Martínez-Monseny, A.F. *et al.* AZATAX: Acetazolamide safety and efficacy in cerebellar syndrome in PMM2 congenital disorder of glycosylation (PMM2-CDG). *Ann Neurol* **85**, 740-751 (2019).
14. Qian, Z., Van den Eynde, J., Heymans, S., Mertens, L. & Morava, E. Vascular ring anomaly in a patient with phosphomannomutase 2 deficiency: A case report and review of the literature. *JIMD Rep* **56**, 27-33 (2020).
15. Jaeken, J. *et al.* Familial psychomotor retardation with markedly fluctuating serum prolactin, FSH and GH levels, partial TBG-deficiency, increased serum arylsulphatase A and increased CSF protein: a new syndrome?: 90. *Pediatric Research* **14**, 179-179 (1980).

16. Trouillas, P. *et al.* International Cooperative Ataxia Rating Scale for pharmacological assessment of the cerebellar syndrome. The Ataxia Neuropharmacology Committee of the World Federation of Neurology. *J Neurol Sci* **145**, 205-11 (1997).
17. Van Schaftingen, E. & Jaeken, J. Phosphomannomutase deficiency is a cause of carbohydrate-deficient glycoprotein syndrome type I. *FEBS Lett* **377**, 318-20 (1995).
18. Ferrer, A. *et al.* Fetal glycosylation defect due to ALG3 and COG5 variants detected via amniocentesis: Complex glycosylation defect with embryonic lethal phenotype. *Mol Genet Metab* **131**, 424-429 (2020).
19. He, P., Ng, B.G., Losfeld, M.E., Zhu, W. & Freeze, H.H. Identification of intercellular cell adhesion molecule 1 (ICAM-1) as a hypoglycosylation marker in congenital disorders of glycosylation cells. *J Biol Chem* **287**, 18210-7 (2012).
20. Eskelinen, E.-L. Roles of LAMP-1 and LAMP-2 in lysosome biogenesis and autophagy. *Molecular Aspects of Medicine* **27**, 495-502 (2006).
21. Radenkovic, S. *et al.* Expanding the clinical and metabolic phenotype of DPM2 deficient congenital disorders of glycosylation. *Molecular Genetics and Metabolism* **132**, 27-37 (2021).
22. Mun, D.G. *et al.* PASS-DIA: A Data-Independent Acquisition Approach for Discovery Studies. *Anal Chem* **92**, 14466-14475 (2020).
23. Zeng, W.F. *et al.* pGlyco: a pipeline for the identification of intact N-glycopeptides by using HCD- and CID-MS/MS and MS3. *Sci Rep* **6**, 25102 (2016).
24. Liu, M.Q. *et al.* pGlyco 2.0 enables precision N-glycoproteomics with comprehensive quality control and one-step mass spectrometry for intact glycopeptide identification. *Nat Commun* **8**, 438 (2017).
25. He, P., Srikrishna, G. & Freeze, H.H. N-glycosylation deficiency reduces ICAM-1 induction and impairs inflammatory response. *Glycobiology* **24**, 392-8 (2014).
26. Medina-Cano, D. *et al.* High N-glycan multiplicity is critical for neuronal adhesion and sensitizes the developing cerebellum to N-glycosylation defect. *Elife* **7**(2018).
27. Yang, B.-B. *et al.* Epalrestat, an Aldose Reductase Inhibitor, Restores Erectile Function in Streptozocin-induced Diabetic Rats. *International Journal of Impotence Research* **31**, 97-104 (2019).
28. Steele, J.W., Faulds, D. & Goa, K.L. Epalrestat. A review of its pharmacology, and therapeutic potential in late-onset complications of diabetes mellitus. *Drugs & Aging* **3**, 532-55 (1993).
29. Sato, K., Yama, K., Murao, Y., Tatsunami, R. & Tampo, Y. Epalrestat increases intracellular glutathione levels in Schwann cells through transcription regulation. *Redox biology* **2**, 15-21 (2013).
30. Hotta, N., Kawamori, R., Fukuda, M. & Shigeta, Y. Long-term clinical effects of epalrestat, an aldose reductase inhibitor, on progression of diabetic neuropathy and other microvascular complications: multivariate epidemiological analysis based on patient background factors and severity of diabetic neuropathy. *Diabet Med* **29**, 1529-33 (2012).
31. Strupczewski, J.D.E., D. B.; Allen, R. C. *Annual Reports in Medicinal Chemistry*, (Elsevier Science, 1993).

FIGURE LEGENDS

FIGURE 1. Epalrestat treatment increased PMM enzyme activity and ICAM-1 protein abundance. A. Epalrestat treatment increased PMM enzyme activity in PMM2-CDG patients' fibroblasts (n=11; P1-P6, P8, P10, P17, P19, P24). The graphs represent results after 10 μM epalrestat treatment for 24 h (P5 responded to the dose of 5 μM epalrestat with 35% increase, P6 did not respond to any of the doses with enzyme activity increase; patient deceased) (Table S2). **B.** Quantification of ICAM-1 protein abundance in immunoblots with PMM2-CDG patients' fibroblasts based on band intensity (p=0.02; n=10; P1-P6, P8, P17, P19, P24). (**C)** Quantification of immunoblots showing LAMP-2 protein abundance in epalrestat untreated and treated patients' fibroblasts (n=10; P1-P6, P8, P17, P19, P24). Epalrestat treatment does not increase LAMP-2 protein abundance. **D.** Immunoblots showing ICAM-1 protein abundance in epalrestat untreated and treated patients' fibroblasts (n=10; P1-P6, P8, P17, P19, P24). Beta-actin was used as a loading control. **E.** Immunoblots showing LAMP-2 protein abundance in epalrestat untreated and treated patients' fibroblasts (n=10; P1-P6, P8, P17, P19, P24). Beta-actin was used as a loading control.

FIGURE 2: Proteomic changes in PMM-deficient patient derived fibroblasts and effect of epalrestat treatment. Panel **A** depicts the waterfall plot of global proteomics of PMM2-CDG and controls. Y-axis is $\log_2$ fold changes (PMM2-CDG/Controls) and X-axis is number of proteins identified. Each individual circle represents a protein. Some of the highly changing representative protein names are marked by triangles and proteins names are provided. **B.** Volcano plot for the same comparison as panel A is shown. X-axis is $\log_2$ fold change (PMM2-CDG/Controls) and Y-axis is the negative logarithm of p value of t-test for significance. Horizontal dashed line marks the cutoff for significance (<0.05) and vertical dashed lines are drawn to highlight the proteins having at least 30% change in either direction (1.3-fold enhancement or reduction). Some of the most significantly changing proteins are marked by triangles and proteins names are provided. **C.** Waterfall plot is depicted for paired comparison of PMM-deficient fibroblasts treated with epalrestat or untreated (vehicle). Y-axis is $\log_2$ fold changes (epalrestat-treated/untreated) and X-axis is number of proteins identified. Each identified protein is depicted with a black circle and some of the highly changing proteins are marked by triangles and proteins names are provided. **D**. Volcano plot is depicted for treated/untreated comparison of PMM-deficient fibroblasts. X-axis depicts $\log_2$ fold change

(treated/untreated) and Y-axis is the negative logarithm of p value of t-test for significance. Horizontal dashed line marks the cutoff for significance (paired t-test, <0.05) and vertical dashed lines are drawn to highlight the proteins having at least 30% change in either direction (1.3-fold enhancement or reduction). Using this cutoff, some of the proteins showing relative higher abundance upon epalrestat treatment are shown as triangles.

FIGURE 3: Glycoproteome alterations in PMM-deficient fibroblasts and remodeling upon epalrestat treatment. A. The waterfall plot of global glycoproteomics of PMM-deficient fibroblasts and controls. Y-axis is $\log_2$ fold changes (PMM2-CDG/Controls) and X-axis is number of unique glycopeptides identified. Each individual triangle represents a unique glycopeptide (unique combination of peptide and glycan structure). Some of the highly changing representative glycopeptides are marked by triangles and glycoprotein names, glycosylation site (N with corresponding amino acid number) and plausible glycan structures are marked. The oval in the lower half (negative Y-axis) of the waterfall plot depicts unique glycopeptides having the plausible glycan structures (shown in the box above the oval), which were reduced in PMM-deficient fibroblasts. **B.** Volcano plot for the given comparison (PMM2-CDG/Controls) is shown. X-axis is $\log_2$ fold change (PMM2-CDG/Controls) and Y-axis is the negative logarithm of p value of t-test for significance. Horizontal dashed line marks the cutoff for significance (<0.05) and vertical dashed lines are drawn to highlight the glycoproteins names having at least 30% change in either direction (1.3-fold enhancement or reduction). Some of the highly changing glycopeptides are marked by triangles and glycoproteins' names, glycosylation sites and plausible glycan structures are drawn. **C.** Waterfall plot is depicted for paired comparative glycoproteomics of PMM-deficient fibroblasts treated with epalrestat or untreated (vehicle). Y-axis is $\log_2$ fold changes (epalrestat-treated/untreated) and X-axis is number of unique glycopeptides identified and quantified. Each unique glycopeptide is depicted with a black circle and some of the altered glycopeptides are marked by triangles and glycoproteins' names, glycosylation sites and plausible glycan structures are marked. **D**. Volcano plot is depicted for treated/untreated comparative glycoproteomics of PMM-deficient fibroblasts. X-axis depicts $\log_2$ fold change (treated/untreated) and Y-axis is the negative logarithm of p value of t-test for significance. Horizontal dashed line marks the cutoff for significance (paired t-test, <0.05) and vertical dashed lines are drawn to highlight the glycopeptides having at least 30% change in

either direction (1.3-fold enhancement or reduction). Using this cutoff, some of the glycopeptides showing enhanced levels upon epalrestat treatment are shown as triangles. With this cutoff none of the unique glycopeptides was found to be reduced.

FIGURE 4. Waterfall plot of two different comparisons at the protein level. A. this panel depicts the waterfall plot of global proteomics of PMM2-CDG and controls. Y-axis is $\log_2$ fold changes (PMM2-CDG/Controls) and X-axis is number of proteins identified. Each individual circle represents a protein name. Some of the highly changing representative proteins are marked by triangles and proteins names are provided. **B.** Waterfall plot is depicted for paired comparison of PMM-deficient fibroblasts treated with epalrestat or untreated (vehicle). Y-axis is $\log_2$ fold changes (epalrestat-treated/untreated) and X-axis is number of proteins identified. Each identified protein is depicted with a black circle and some of the highly changing proteins are marked by triangles and proteins names are provided. These waterfall plots are shown side-by-side for comparison.

FIGURE 5. Glycopeptides with the highest improvement (%) after epalrestat treatment. Epalrestat treated (solid line) and untreated (dashed line) PMM2-CDG patient-derived fibroblasts were compared to controls and ten glycopeptides showed the highest percent of improvement in their relative abundance levels are shown in this figure. Every datapoint is one glycopeptide and their corresponding protein name, glycosylation site, and plausible glycan structure are marked at the bottom.

FIGURE 6. Urine sorbitol and mannitol concentrations in patients with peripheral neuropathy, liver pathology, and CDG phenotype. Concentrations were normalized to urine creatine concentration. Significant variation in urine sorbitol and mannitol concentrations were associated with both peripheral neuropathy score and liver pathology score, with elevated urine sorbitol and mannitol detected in CDG patients displaying both moderate neuropathy and mild liver pathology. Krukal-Wallis test followed by Dunn's multiple comparisons test (**A, C**) and Mann Whitney test (**B, D**). Data are expressed as mean±SD. $p<0.05$(*), $p<0.01$(**), $p<0.001$(**). Urine sorbitol levels positively correlated with severe CDG phenotype ($r=0.5$,

p<0.02) (**E**). There was no correlation with the mild or moderate category. Urine mannitol levels did not correlate with mild, moderate, or severe categories based on NPCRS scores (**F**).

FIGURE 7. Epalrestat has a positive effect on the glycosylation defect, growth, and normalization of elevated sorbitol and mannitol levels in the PMM2-CDG pediatric patient. **A.** BMI of the patient increased substantially following epalrestat treatment. **B.** Pharmacokinetics profile shows rapid elimination of epalrestat. The samples representing each time point were taken from different dosing days. Epalrestat was eliminated with a t½ of ~1-2 hours. Blood samples were provided were drawn: prior to therapy (0 h) and 1h post-dose (month 6), 1h 20min (day 1), 1h 40min (day 90), 2h (month 9), 3h (day 30), 4h (day 2), 6h (month 12), 8h 30min (day epalrestat was eliminated with a t½ of ~1-2 hours. A peak concentration of epalrestat in blood was 1125.408 ng/ml (or 3.5 μM) 1 hour after the epalrestat administration. A trough level as the lowest concentration reached by epalrestat before the next dose was 23.392 ng/ml after 8 hours. P1 single-dose PK data on 0.27 mg/kg epalrestat dose three times **C.** Urine sorbitol level before starting epalrestat therapy (sorbitol = 19.93 mmol/mol creatinine), after 3-month (5.78 mmol/mol creatinine) and 6 months of therapy (6.20 mmol/mol creatinine) compared to controls (<5 mmol/mol creatinine) **D.** Urine mannitol level before starting epalrestat therapy (mannitol = 648.6 mmol/mol creatinine), after 3-month (37.32 mmol/mol creatinine) and 6 months of therapy (25.09 mmol/mol creatinine) compared to controls (<20mmol/mol creatinine). **E.** Increasing weight during epalrestat therapy and decreasing blood transferrin glycoform ratio analysis 12 months prior to therapy and during 12 months of epalrestat therapy. Normal level for Mono-oligo/Di-oligo Controls: Ratio ≤ 0.06 and A-oligo/Di-oligo Controls: Ratio ≤ 0.01.

FIGURE 8. Hypothetical mechanism of altered polyol metabolism in PMM2-CDG. Decrease in PMM enzyme activity is associated with an excess of metabolites including sorbitol and mannitol.

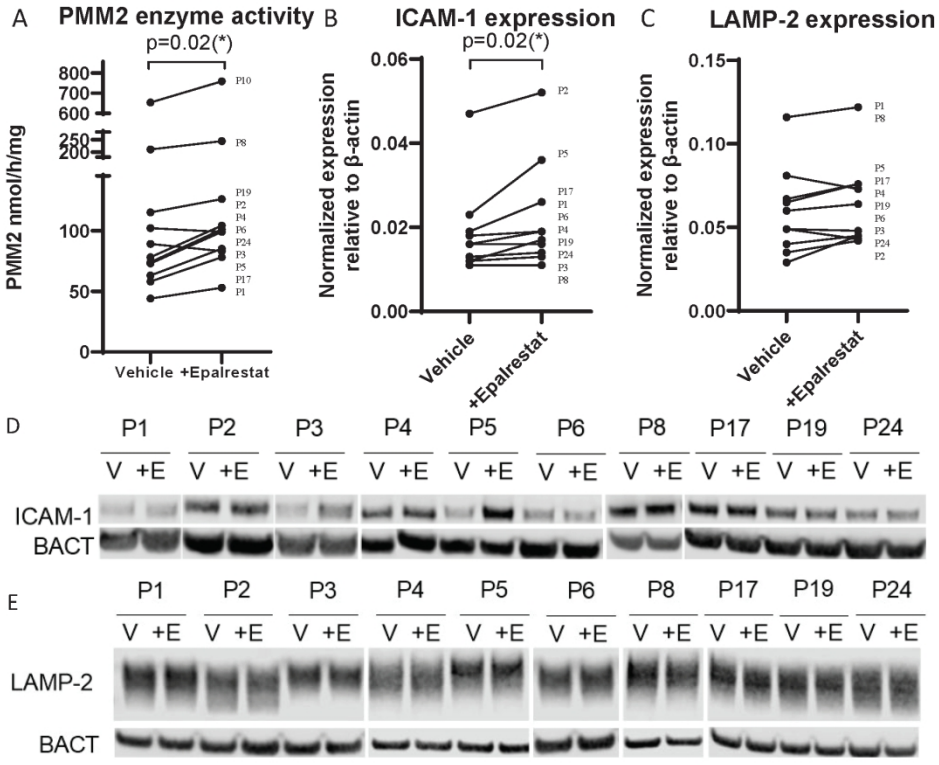

FIGURE 1. Epalrestat treatment increased PMM enzyme activity and ICAM-1 protein abundance. A. Epalrestat treatment increased PMM enzyme activity in PMM2-CDG patients' fibroblasts (n=11; P1-P6, P8, P10, P17, P19, P24). The graphs represent results after 10 μM epalrestat treatment for 24 h (P5 responded to the dose of 5 μM epalrestat with 35% increase, P6 did not respond to any of the doses with enzyme activity increase; patient deceased) (Table S2). B. Quantification of ICAM-1 protein abundance in immunoblots with PMM2-CDG patients' fibroblasts based on band intensity (p=0.02; n=10; P1-P6, P8, P17, P19, P24). (C) Quantification of immunoblots showing LAMP-2 protein abundance in epalrestat untreated and treated patients' fibroblasts (n=10; P1-P6, P8, P17, P19, P24). Epalrestat treatment does not increase LAMP-2 protein abundance. D. Immunoblots showing ICAM-1 protein abundance in epalrestat untreated and treated patients' fibroblasts (n=10; P1-P6, P8, P17, P19, P24). Beta-actin was used as a loading control. E. Immunoblots showing LAMP-2 protein abundance in epalrestat untreated and treated patients' fibroblasts (n=10; P1-P6, P8, P17, P19, P24). Beta-actin was used as a loading control.

170x138mm (300 x 300 DPI)

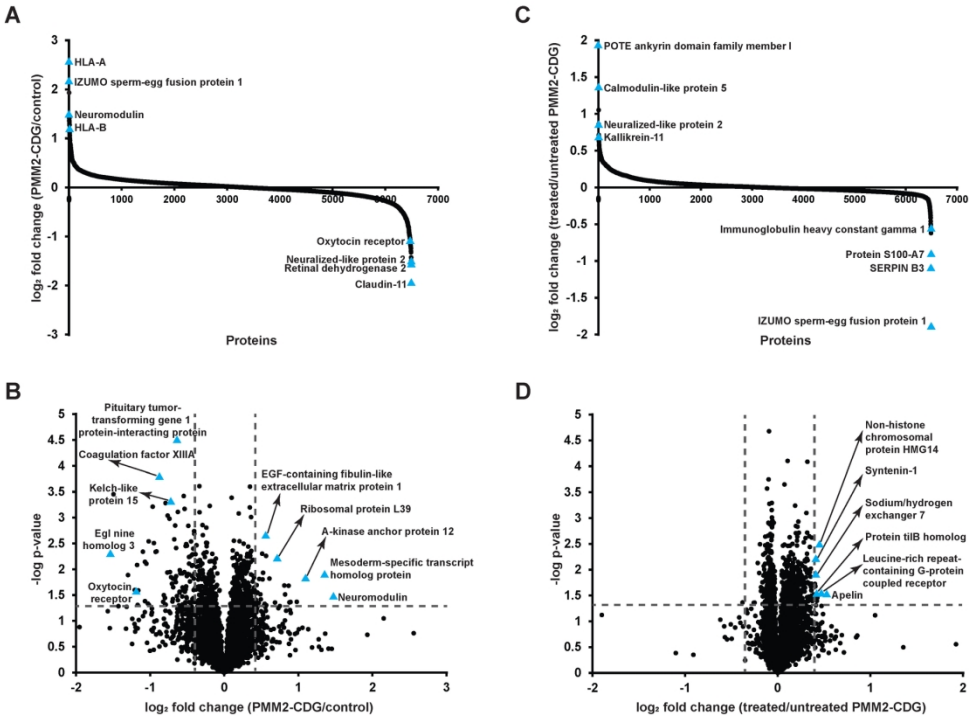

FIGURE 2: Proteomic changes in PMM-deficient patient derived fibroblasts and effect of epalrestat treatment. Panel A depicts the waterfall plot of global proteomics of PMM2-CDG and controls. Y-axis is log2 fold changes (PMM2-CDG/Controls) and X-axis is number of proteins identified. Each individual circle represents a protein. Some of the highly changing representative protein names are marked by triangles and proteins names are provided. B. Volcano plot for the same comparison as panel A is shown. X-axis is log2 fold change (PMM2-CDG/Controls) and Y-axis is the negative logarithm of p value of t-test for significance. Horizontal dashed line marks the cutoff for significance (<0.05) and vertical dashed lines are drawn to highlight the proteins having at least 30% change in either direction (1.3-fold enhancement or reduction). Some of the most significantly changing proteins are marked by triangles and proteins names are provided. C. Waterfall plot is depicted for paired comparison of PMM-deficient fibroblasts treated with epalrestat or untreated (vehicle). Y-axis is log2 fold changes (epalrestat-treated/untreated) and X-axis is number of proteins identified. Each identified protein is depicted with a black circle and some of the highly changing proteins are marked by triangles and proteins names are provided. D. Volcano plot is depicted for treated/untreated comparison of PMM-deficient fibroblasts. X-axis depicts log2 fold change (treated/untreated) and Y-axis is the negative logarithm of p value of t-test for significance. Horizontal dashed line marks the cutoff for significance (paired t-test, <0.05) and vertical dashed lines are drawn to highlight the proteins having at least 30% change in either direction (1.3-fold enhancement or reduction). Using this cutoff, some of the proteins showing relative higher abundance upon epalrestat treatment are shown as triangles.

170x138mm (300 x 300 DPI)

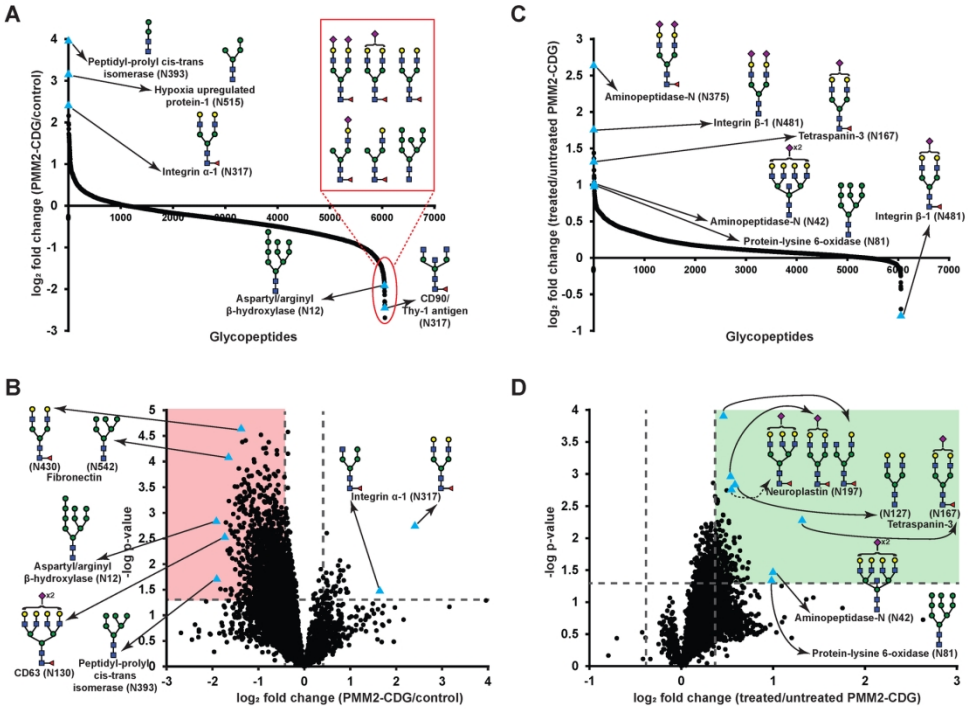

FIGURE 3: Glycoproteome alterations in PMM-deficient fibroblasts and remodeling upon epalrestat treatment. A. The waterfall plot of global glycoproteomics of PMM-deficient fibroblasts and controls. Y-axis is log2 fold changes (PMM2-CDG/Controls) and X-axis is number of unique glycopeptides identified. Each individual triangle represents a unique glycopeptide (unique combination of peptide and glycan structure). Some of the highly changing representative glycopeptides are marked by triangles and glycoprotein names, glycosylation site (N with corresponding amino acid number) and plausible glycan structures are marked. The oval in the lower half (negative Y-axis) of the waterfall plot depicts unique glycopeptides having the plausible glycan structures (shown in the box above the oval), which were reduced in PMM-deficient fibroblasts. B. Volcano plot for the given comparison (PMM2-CDG/Controls) is shown. X-axis is log2 fold change (PMM2-CDG/Controls) and Y-axis is the negative logarithm of p value of t-test for significance. Horizontal dashed line marks the cutoff for significance (<0.05) and vertical dashed lines are drawn to highlight the glycoproteins names having at least 30% change in either direction (1.3-fold enhancement or reduction). Some of the highly changing glycopeptides are marked by triangles and glycoproteins' names, glycosylation sites and plausible glycan structures are drawn. C. Waterfall plot is depicted for paired comparative glycoproteomics of PMM-deficient fibroblasts treated with epalrestat or untreated (vehicle). Y-axis is log2 fold changes (epalrestat-treated/untreated) and X-axis is number of unique glycopeptides identified and quantified. Each unique glycopeptide is depicted with a black circle and some of the altered glycopeptides are marked by trianglesand glycoproteins' names, glycosylation sites and plausible glycan structures are marked. D. Volcano plot is depicted for treated/untreated comparative glycoproteomics of PMM-deficient fibroblasts. X-axis depicts log2 fold change (treated/untreated) and Y-axis is the negative logarithm of p value of t-test for significance. Horizontal dashed line marks the cutoff for significance (paired t-test, <0.05) and vertical dashed lines are drawn to highlight the glycopeptides having at least 30% change in either direction (1.3-fold enhancement or reduction). Using this cutoff, some of the glycopeptides showing enhanced levels upon epalrestat treatment are shown as triangles. With this cutoff none of the unique glycopeptides was found to be reduced.

170x138mm (300 x 300 DPI)

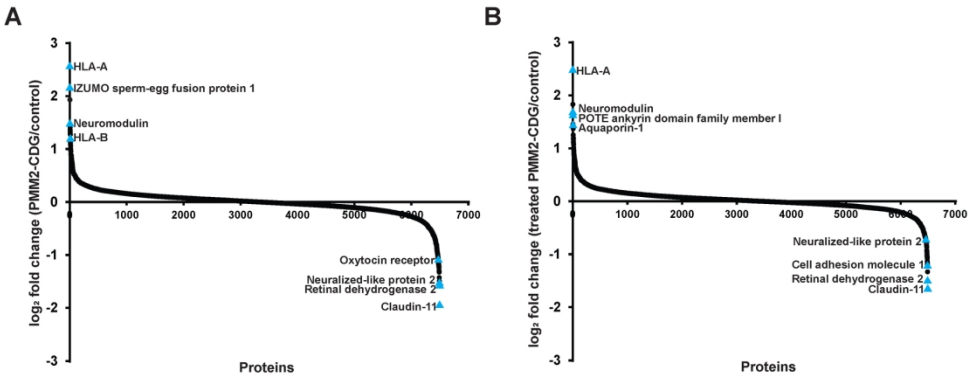

FIGURE 4. Waterfall plot of two different comparisons at the protein level. A. this panel depicts the waterfall plot of global proteomics of PMM2-CDG and controls. Y-axis is log2 fold changes (PMM2-CDG/Controls) and X-axis is number of proteins identified. Each individual circle represents a protein names. Some of the highly changing representative proteins are marked by triangles and proteins names are provided. B. Waterfall plot is depicted for paired comparison of PMM-deficient fibroblasts treated with epalrestat or untreated (vehicle). Y-axis is log2 fold changes (epalrestat-treated/untreated) and X-axis is number of proteins identified. Each identified protein is depicted with a black circle and some of the highly changing proteins are marked by triangles and proteins names are provided. These waterfall plots are shown side-by-side for comparison.

170x138mm (300 x 300 DPI)

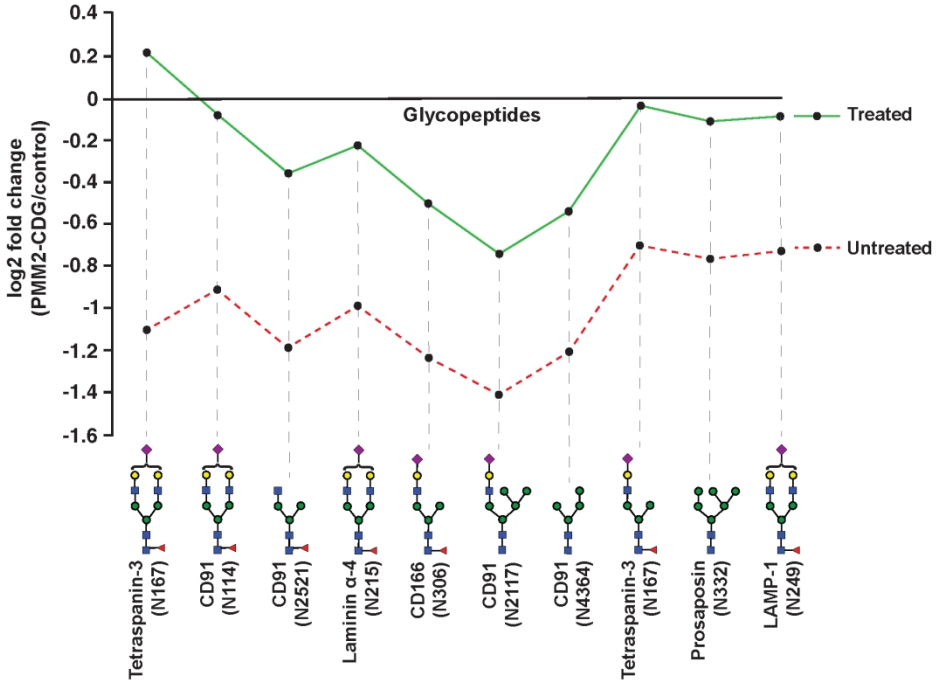

FIGURE 5. Glycopeptides with the highest improvement (%) after epalrestat treatment. Epalrestat treated (solid line) and untreated (dashed line) PMM2-CDG patient-derived fibroblasts were compared to controls and ten glycopeptides showed the highest percent of improvement in their relative abundance levels are shown in this figure. Every datapoint is one glycopeptide and their corresponding protein name, glycosylation site, and plausible glycan structure are marked at the bottom.

170x138mm (300 x 300 DPI)

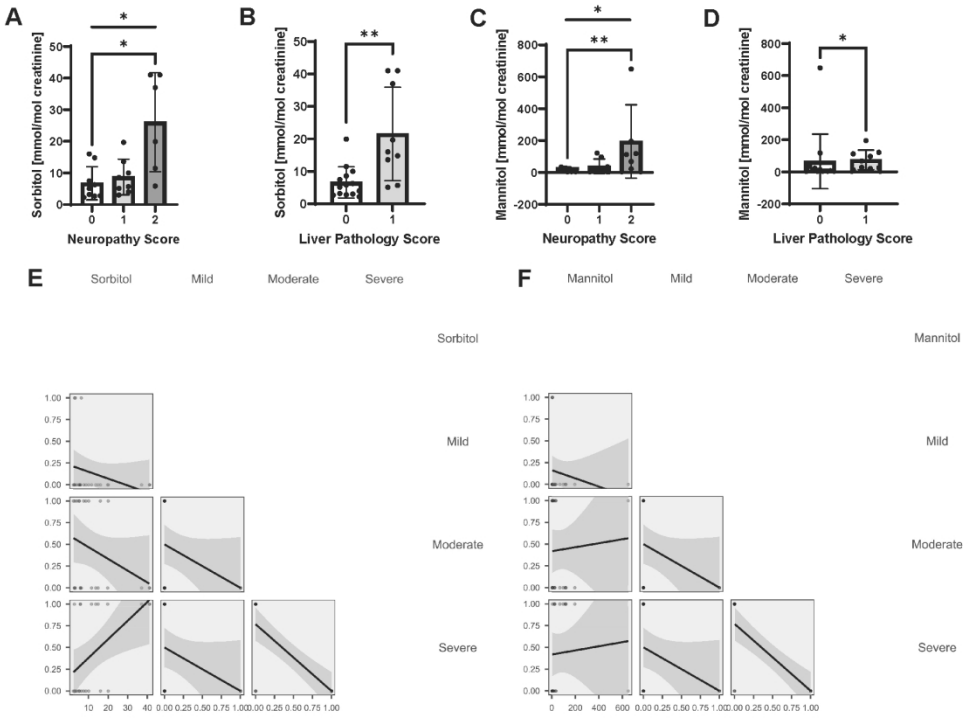

FIGURE 6. Urine sorbitol and mannitol concentrations in patients with peripheral neuropathy, liver pathology, and CDG phenotype. Concentrations were normalized to urine creatine concentration. Significant variation in urine sorbitol and mannitol concentrations were associated with both peripheral neuropathy score and liver pathology score, with elevated urine sorbitol and mannitol detected in CDG patients displaying both moderate neuropathy and mild liver pathology. Krukal-Wallis test followed by Dunn's multiple comparisons test (A, C) and Mann Whitney test (B, D). Data are expressed as mean±SD. $p<0.05$(*), $p<0.01$(**), $p<0.001$(**). Urine sorbitol levels positively correlated with severe CDG phenotype ($r=0.5$, $p<0.02$) (E). There was no correlation with the mild or moderate category. Urine mannitol levels

did not correlate with mild, moderate, or severe categories based on NPCRS scores (F).

170x138mm (300 x 300 DPI)

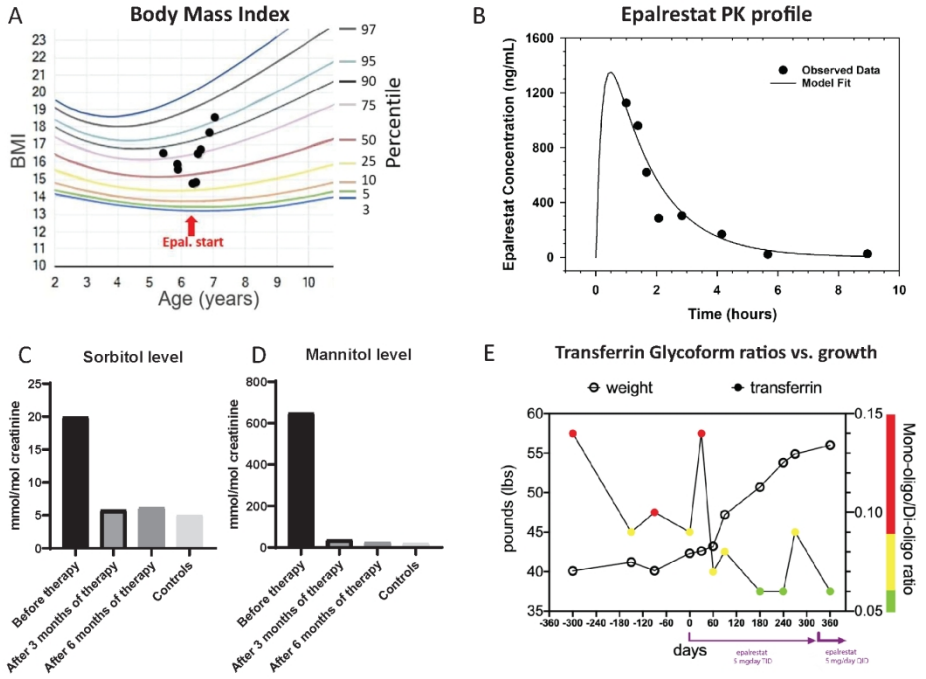

FIGURE 7. Epalrestat has a positive effect on the glycosylation defect, growth, and normalization of elevated sorbitol and mannitol levels in the PMM2-CDG pediatric patient. A. BMI of the patient increased substantially following epalrestat treatment. B. Pharmacokinetics profile shows rapid elimination of epalrestat. The samples representing each time point were taken from different dosing days. Epalrestat was eliminated with a t½ of ~1-2 hours. Blood samples were provided were drawn: prior to therapy (0 h) and 1h post-dose (month 6), 1h 20min (day 1), 1h 40min (day 90), 2h (month 9), 3h (day 30), 4h (day 2), 6h (month 12), 8h 30min (day epalrestat was eliminated with a t½ of ~1-2 hours. A peak concentration of epalrestat in blood was 1125.408 ng/ml (or 3.5 μM) 1 hour after the epalrestat administration. A trough level as the lowest concentration reached by epalrestat before the next dose was 23.392 ng/ml after 8 hours. P1 single-dose PK data on 0.27 mg/kg epalrestat dose three times C. Urine sorbitol level before starting epalrestat therapy (sorbitol = 19.93 mmol/mol creatinine), after 3-month (5.78 mmol/mol creatinine) and 6 months of therapy (6.20 mmol/mol creatinine) compared to controls (<5 mmol/mol creatinine) D. Urine mannitol level before starting epalrestat therapy (mannitol = 648.6 mmol/mol creatinine), after 3-month (37.32 mmol/mol creatinine) and 6 months of therapy (25.09 mmol/mol creatinine) compared to controls (<20mmol/mol creatinine). E. Increasing weight during epalrestat therapy and decreasing blood transferrin glycoform ratio analysis 12 months prior to therapy and during 12 months of epalrestat therapy. Normal level for Mono-oligo/Di-oligo Controls: Ratio ≤ 0.06 and A-oligo/Di-oligo Controls: Ratio ≤ 0.01.

170x138mm (300 x 300 DPI)

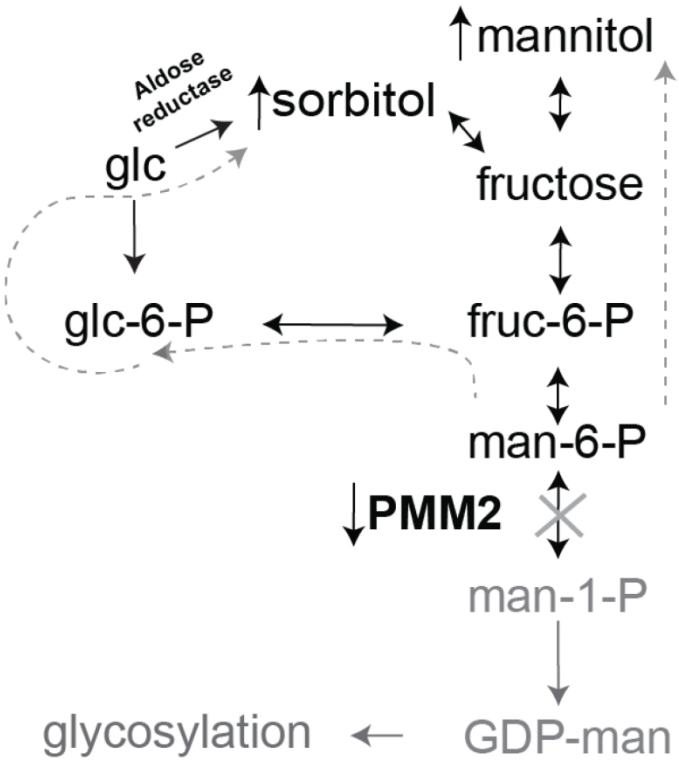

FIGURE 8. Hypothetical mechanism of altered polyol metabolism in PMM2-CDG. Decrease in PMM enzyme activity is associated with an excess of metabolites including sorbitol and mannitol.

170x138mm (300 x 300 DPI)

Supplementary Table S1. General information for 24 individuals with PMM2-CDG. Data includes all patients enrolled for clinical data collection (P1-P24), polyols quantification (P1-P5, P7-P24), included in the *in vitro* studies (P1-P6, P8, P10, P17, P19, P24), and the evaluation of safety and efficacy of epalrestat and sorbitol and mannitol excretion investigation (P1)**.**
*Abnormal sorbitol and mannitol levels are bold (sorbitol: controls <5 mmol/mol creatinine; mannitol: controls <20 mmol/mol creatinine). P1was reported by Qian et al 2020.; twins P4 and P5 were reported by Jaeken et al. 1980.

No.	P1	P2	P3	P4	P5	P6	P7	P8	P9	P10	P11	P12
Pathogenic variant	c.422G>A, c.415G>A	c.422G>A, c.548T>C	c.422G>A, c.647A>T	c.422G>A, c.338C>T	c.422G>A, c.338C>T	c.124A>G, c.338C>T	c.422G>A, c.357C>A	c.422G>A, c.203T>G	c.109C>T, c.337C>A	c.98A>C, c.140C>T	c.422G>A, c.722G>C	c.422G>A, c.458T>C
Age/Gender	6/F	6/M	7/M	44/F	44/F	7/M †	7/M	1/M	2/M	8/M	12/M	16/M
NPCRS Section I: Current Function 1. Vision	++	-	-	+	+	+++	+	-	-	-	-	-
2. Hearing	-	-	+	-	-	-	++	-	-	-	-	-
3. Communication	++	+	++	++	++	+	++	++	+	+	+	+
4. Feeding	-	-	+	+	+	+++	++	-	-	-	-	-
5. Self-care	+++	+++	++	++	++	+++	+++	+++	+++	++	+	+
6. Mobility	+++	++	++	+++	+++	+++	+++	++	+++	+++	+	++
7. Educational achievement	+	+	+	++	++	++	++	++	++	+	+	++
NPCRS Section II: System Specific Involvement 1. Seizures	-	-	-	-	-	+	+++	-	+	-	-	-
2. Encephalopathy	-	-	-	-	-	+	+	+	-	-	-	-
3. Bleeding diathesis or coagulation defects	-	+	+	+	+	++	-	-	+	+	-	+
4. Gastrointestinal	-	-	+	+	+	+	-	-	+	-	-	+++
5. Endocrine	-	-	++	+	+	+	-	-	-	-	-	-
6. Respiratory	-	-	-	-	-	-	-	-	-	-	-	-
7. Cardiovascular (over preceding 12 months)	-	-	-	-	+	-	-	-	-	-	-	+

8. Renal	-	-	-	-	-	+++	-	-	-	-	-	-
9. Liver	-	-	+	+	+	+	+	+	+	-	-	-
10. Blood	-	-	-	-	-	+++	-	-	-	+	-	-
NPCRS Section III: Current Clinical Assessment 1. Growth	-	-	+	+	+	-	+	+	+	+	-	-
2. Development over preceding 6 months	5	5	5	6	5	10	5	5	5	5	5	5
3. Vision with usual glasses.	+	+	+	+	+	+++	+	-	-	-	-	-
4. Strabismus and eye movement	+	+	++	+	+	+	+	+	+	+	-	-
5. Myopathy	++	+	+	++	++	-	+	+	++	+	+	+
6. Ataxia	++	++	++	++	++	+++	++	+	-	++	++	++
7. Pyramidal	-	-	-	-	+	-	+	-	-	++	-	-
8. Extrapyramidal	-	-	-	-	-	-	++	+	-	+	-	-
9. Neuropathy	++	-	+	++	++	-	++	-	-	+	-	+
Section I: Current Function; Total = 21	11	7	9	11	11	15	15	9	9	7	4	6
Section II: System Specific Involvement; Total = 30	0	1	5	4	5	13	5	2	3	2	0	5
Section III: Current Clinical Assessment; Total = 31	13	10	13	15	15	17	15	10	9	14	8	9
Total = 82; Mild (0–14), moderate (15–25) and severe (>26)	24	18	27	30	31	45	35	21	21	22	12	20
Sorbitol	**19.9**	**6.27**	**5.67**	**41**	**41**	N/A	**37**	**5.11**	**16**	3	3.19	3.99
Mannitol	**649**	5.35	**122**	**69**	**113**	N/A	**195**	13.8	**25**	6	4.65	3.64
Condition	Moderate	Moderate	Severe	Severe	Severe	Severe	Severe	Moderate	Moderate	Moderate	Mild	Moderate

*age at the time of the publication; N/A- not applicable; + symptom present (+ mild, ++ moderate, +++ severe), - normal/absent, † deceased.

No.	P13	P14	P15	P16	P17	P18	P19	P20	P21	P22	P23	P24

Pathogenic variant	c.368G>A, c.722G>C	c.647A>G, c.415G>A	c.422 G>A, c.640-23A>G	c.422 G>A, c.640-23A>G	c.422G>A, c.338C>T	c.563A>G, c.691G>A	c.422 G>A, c.385G>A	c.422G>A, c.357C>A	c.422G>A, c.385G>A	c.422G>A, c.691G>A	c.422G>A, c.713G>A	c.422G>A, c.623G>C
Age/Gender	22/F	70/M	11/F	9/M	7/M	8/F	5/M	3/M	4/F	4/M	8/M	10/F
NPCRS Section I: Current Function 1. Vision	-	-	+	+	-	+	-	-	-	+	+	-
2. Hearing	-	++	++	-	-	++	-	-	-	-	-	-
3. Communication	+	-	-	+	++	+	++	++	++	++	+	++
4. Feeding	-	-	-	+	-	-	++	++	-	++	++	+++
5. Self-care	+	-	++	++	+	+	++	+++	+++	+++	-	+++
6. Mobility	+	+	++	++	++	++	++	++	++	+++	-	+++
7. Educational achievement	+	-	++	++	++	++	++	+	++	++	-	++
NPCRS Section II: System Specific Involvement 1. Seizures	-	-	+	++	+	-	+	-	+	+	-	-
2. Encephalopathy	-	-	-	-	-	-	-	-	-	-	-	-
3. Bleeding diathesis or coagulation defects	-	-	-	-	+	+	+	+	+	+	-	+
4. Gastrointestinal	+	+	+	+	-	-	+	+	-	+	++	-
5. Endocrine	++	-	++	-	-	-	++	++	-	-	++	+
6. Respiratory	-	+	-	+	-	-	-	-	-	-	-	-
7. Cardiovascular (over preceding 12 months)	-	-	-	-	-	+	++	-	+	-	-	-
8. Renal	-	-	-	-	-	+	-	-	-	-	-	-
9. Liver	-	-	-	-	-	-	+	+	-	+	-	-
10. Blood	-	-	-	-	-	-	-	+	-	-	+	++
NPCRS Section III: Current Clinical Assessment 1. Growth	+	-	-	+	-	-	+	+	+	+	+	+++
2. Development over preceding 6 months	5	-	5	5	5	5	5	5	5	5	5	6
3. Vision with usual glasses.	-	-	+	+	-	+	-	-	-	+	+	-

4. Strabismus and eye movement	-	+	++	+	+	-	++	+	+	-	-	++
5. Myopathy	+	-	+	+	+	+	-	+	-	++	-	++
6. Ataxia	+	++	++	++	++	++	+++	++	++	++	+	+++
7. Pyramidal	-	-	-	-	-	+	-	-	-	++	-	-
8. Extrapyramidal	-	-	-	+	-	+	-	+	+	++	-	-
9. Neuropathy	-	-	++	++	+	+	-	+	+	+	-	-
Section I: Current Function; Total = 21	4	3	9	9	7	9	10	10	9	13	5	13
Section II: System Specific Involvement; Total = 30	3	2	4	4	2	3	8	6	3	4	5	4
Section III: Current Clinical Assessment; Total = 31	8	3	13	15	10	11	11	12	11	16	9	16
Total = 82; Mild (0–14), moderate (15–25) and severe (>26)	15	8	26	28	19	23	29	28	23	33	19	33
Sorbitol	2.24	2.8	**5.86**	**11.5**	**5.16**	**10**	**14.8**	**13.6**	**8.61**	**19.7**	**7.47**	2.69
Mannitol	4.75	7.99	**22.5**	**119**	6.96	14	**28.5**	**97.5**	**35.5**	**21.1**	**33.5**	7.03
Condition	Moderate	Mild	Severe	Severe	Moderate	Moderate	Severe	Severe	Moderate	Severe	Moderate	Severe

*age at the time of the publication; N/A- not applicable; + symptom present (+ mild, ++ moderate, +++ severe), - normal/absent, † deceased.

Supplementary Table S2. Treatment with three different doses of epalrestat in fibroblast of PMM2-CDG individuals.

*The highest fold changes are bold.

Epalrestat with three different doses, PMM activity (nmol/h/mg)						
Subjects, P=11	Baseline	Fold change: 5 µM Epalrestat	Fold change: 10 µM Epalrestat	Fold change: 20 µM Epalrestat	The best dose	The highest fold change
P1	1	**1.43**	1.2	1.2	5 µM	**1.43**
P2	1	1.01	**1.33**	0.7	10 µM	**1.33**
P3	1	0.86	**1.35**	0.9	10 µM	**1.35**
P4	1	1.26	1.36	**1.5**	10 µM	**1.36**
P5	1	**1.35**	0.93	0.9	5 µM	**1.35**
P6	1	0.98	0.97	0.6	-	-
P8	1	1.07	**1.16**	1.1	10 µM	**1.16**
P10	1	**1.22**	1.16	1.2	5 µM	**1.22**
P17	1	0.9	0.75	**1.1**	20 µM	**1.1**
P19	1	0.84	1.1	**1.2**	20 µM	**1.2**
P24	1	0.78	**1.36**	0.9	10 µM	**1.36**

Supplementary Table S3. Blood transferrin glycoform ratio analysis by mass spectrometry 12 months prior to therapy and during 12 months treatment with 0.8 mg/kg/day (15 mg/day) epalrestat (Ono Pharmaceuticals, Osaka, Japan) in a single PMM2-CDG patient.

Carbohydrate Deficient Transferrin for CDG		
Time of sampling	Mono-oligo/Di-oligo	A-oligo/Di-oligo
1 y. prior trial	**0.14**	0.01
6 m. prior trial	**0.09**	0.003
3 m. prior trial	**0.10**	0.007
Prior first dose	**0.09**	0.005
1st month	**0.14**	0.005
2nd month	**0.07**	0.01
3rd month	**0.08**	0.004
6th month	0.06	0.003
8th month	0.06	0.004
9th month	**0.09***	0.004
12th month	0.06	0.004

Controls: Mono-oligo/Di-oligo Controls: Ratio ≤ 0.06 and A-oligo/Di-oligo Controls: Ratio ≤ 0.01
*Patient has been underdosed due to unexpected weight gain, with dose correction to 0.8 mg/kg/day at 11 months. Abnormal values are in bold.